Nanoscale

High Performance Photothermal Film with Spherical Shell-type Metallic Nanocomposites for Solar Thermoelectric Conversion

Journal:	*Nanoscale*
Manuscript ID:	NR-COM-02-2015-000943.R1
Article Type:	Communication
Date Submitted by the Author:	12-Mar-2015

Complete List of Authors:	Kosuga, Atsuko; Osaka Prefecture University, Nanoscience and Nanotechnology Research Center Yamamoto, Yasuyuki; Osaka Prefecture University, Department of Physical Science, Graduate School of Science; Osaka Prefecture University, Department of Physics and Electronics, Graduate School of Engineering Miyai, Moe; Osaka Prefecture University, Department of Physical Science, Graduate School of Science Matsuzawa, Mie; Osaka Prefecture University, Nanoscience and Nanotechnology Research Center Nishimura, Yushi; Osaka Prefecture University, Department of Physical Science, Graduate School of Science; Osaka Prefecture University, Department of Physics and Electronics, Graduate School of Engineering Hidaka, Shimpei; Osaka Prefecture University, Nanoscience and Nanotechnology Research Center; Osaka Prefecture University, Department of Physics and Electronics, Graduate School of Engineering Yamamoto, Kohei; Osaka Prefecture University, Nanoscience and Nanotechnology Research Center; Osaka Prefecture University, Department of Physics and Electronics, Graduate School of Engineering Tanaka, Shin; Osaka Prefecture University, Nanoscience and Nanotechnology Research Center; Osaka Prefecture University, Department of Physics and Electronics, Graduate School of Engineering Yamamoto, Yojiro; GreenChem Inc., Tokonami, Shiho; Osaka Prefecture University, Nanoscience and Nanotechnology Research Center Iida, Takuya; Osaka Prefecture University, Department of Physical Science, Graduate School of Science

Journal Name

Nanoscale

Dynamic Article Links ►

Cite this: DOI: 10.1039/c0xx00000x

www.rsc.org/xxxxxx

ARTICLE TYPE

High Performance Photothermal Film with Spherical Shell-type Metallic Nanocomposites for Solar Thermoelectric Conversion

Atsuko Kosuga,[a,*] Yasuyuki Yamamoto,[b,c] Moe Miyai,[b] Mie Matsuzawa,[a] Yushi Nishimura,[b,c] Shimpei Hidaka,[a,c] Kohei Yamamoto,[a,c] Shin Tanaka,[a,c] Yojiro Yamamoto,[d] Shiho Tokonami[a] and Takuya Iida[a,b,*]

Received (in XXX, XXX) Xth XXXXXXXXX 20XX, Accepted Xth XXXXXXXXX 20XX
DOI: 10.1039/b000000x

A photothermal film (PTF) with densely assembled gold nanoparticle-fixed beads on a polymer substrate is fabricated. Remarkably, temperature rise higher than 40 °C is achieved in the PTF with only 100 seconds solar irradiation, and output power of thermoelectric device was enhanced to be one order higher than that without PTF. These results will pioneer a rapid solar thermoelectric devices.

Power generation technology using solar energy is expected to play an important role in the field of sustainable energy in the future. Generally speaking, there are two methods of converting solar energy directly into electricity using energy materials: through photovoltaic (PV) materials based on the photoelectric effect,[1] and thermoelectric (TE) materials based on the Seebeck effect.[2] While the former approach has already been put into widespread use, the latter has recently become the focus of considerable attention as a cutting-edge research topic. Since the conversion efficiency of a TE device is proportional to the temperature difference across the device, a key challenge for solar TE generation is producing a significant temperature difference across a device with a low solar heat flux. A number of studies have approached this problem by concentrating solar heat on the hot junction of a TE device, using mirrors or lenses to create a large temperature difference.[3-5] Such a concentration of heat in solar TE devices generally requires solar tracking and additional systems, increasing the overall system size and complexity. Kraemer et al. recently reported the development of a promising solar TE device in a flat-panel absorber configuration, and achieved a peak efficiency of 4.6 % under AM 1.5G conditions.[6] This demonstrated a potentially highly-efficient solar absorber and also made a critical contribution towards the realization of a cost-effective, highly-distributed solar TE generation system.

As a physical mechanism to enhance the absorption of white light, the localized surface plasmon (LSP) in a metallic nanostructure[7,8] has attracted the attention of many researchers in various optical technologies and biological science. This is because a LSP has a relatively broad optical spectrum with large oscillator strength in the visible wavelength region due to the nanoscale confinement of free electrons although a bulk metal usually shows a high reflection of white light and a weak photothermal effect. In the field of PV devices, the strong light scattering from a LSP is considered to be a promising mechanism for enhancement of the photoelectric effect.[9] As regards TE devices, the efficient white light absorption by a LSP, which leads to heat generation, is a key component in highly efficient solar TE applications. Focusing on the collective phenomena of LSPs in metallic nanoparticles (NPs), the significantly large broadening of the scattering spectrum can be expected to enhance the solar absorption due to plasmonic superradiance. This occurs through optical assembling of NPs into a two-dimensional plasmonic light harvesting system, which was theoretically predicted[10] and has been experimentally demonstrated.[11] Meanwhile, a recent advance in the chemical self-assembling method (CSAM) enables us to create a three-dimensional assembled structure of a vast number of metallic NPs on a plastic bead via binder organic molecules, using a low cost and simple mixing method.[12] Previously, it was reported that a metallic NP-fixed bead (MNFB) fabricated by this CSAM exhibits dramatic spectral broadening in the wavelength region, ranging from ultraviolet (UV) to infrared (IR) light, and a large red-shift in the order of several hundred nanometers if the NP density is increased using small binders.[13] In addition, a prominent spectral modulation of MNFB has been used for application in DNA detection under white light irradiation.[14] Also, under IR laser irradiation, high density metallic NPs can generate a high photothermal effect and kill pathogenic cells,[15] and a protein was detected by laser-induced heat of MNFB.[16] However, there were no report on the photothermal effect arising from MNFBs being used as sunlight absorbers, through a mechanism based on the collective phenomena of LSP behaviour under broadband white light irradiation.

Here, in order to pursue the potential use of plasmonic collective

phenomena in TE applications, we have fabricated highly-efficient broadband photothermal films (PTF) consisting of densely-assembled MNFBs composed of gold or silver NPs (AuNPs or AgNPs). That is, the MNFBs contain AuNP-fixed beads (AuNP-FBs) or AgNP-fixed beads (Ag NP-FBs) deposited on a transparent polymer film through a simple drop-and-dry method. We then investigated the photothermal effect of the fabricated PTFs and the potential application of the broadband PTF in a TE conversion system.

A polyethylene naphthalate (PEN) film (Teonex®, Q65F, Teijin-DuPont Films, Japan) was used as a transparent substrate (thickness: 100 μm, dimensions: 4 × 4 cm^2, cut from a large film) after washing with ethanol and drying with blowing nitrogen gas. Then, 2 mL of a MNFB aqueous suspension (AuNP-FB: ~300 Au NPs of approximately 37.5 nm diameter or AgNP-FB: ~8000 Ag NPs of approximately 7.4 nm diameter, on acrylate resin beads of 400-nm diameter) with 11-amino-1-undecanethiol[13,14] (2.49 × 10^{10} beads/mL) was uniformly painted on the PEN film using a micropipette on a 3 × 3 cm^2 region of two sheets of PEN film, without masking tape. The films were then naturally dried for a period of about 12 h in a vacuum desiccator. After drying, these films were pasted together at the painted regions by applying double-stick tapes at the two sides. A schematic image of a completed PTF can be seen as part of Figure 1 (a). Also, in order to investigate the surface conditions of the PTFs, a scanning electron microscope (SEM) was used and it was confirmed that a vast number of AuNP-FBs or AgNP-FBs were densely and uniformly assembled on a PEN film coated with a thin conductive layer of indium tin oxide (ITO), respectively (Figure 1 (b) and (c)). The photothermal properties of our developed PTFs were determined using a solar simulator (XES-40S1, San-Ei Electric, Japan) that can generate artificial sunlight of 1SUN (100 mW/cm^2), at AM 1.5 G, while the temperature of the PTF surfaces were measured using a thermocouple connected to a digital multimeter (7352A, ADCMT, Japan). In order to measure the pure photothermal effect from the PTFs while avoiding heat dissipation into the sample stage, the experimental set up was constructed using a homemade transparent plastic framework (lower panel in Figure 1(a)).

First, the extinction spectra of the AuNP-FB and AgNP-FB aqueous suspensions, and those of the single AuNPs and AgNPs before fixation, were observed using a UV–vis spectrophotometer (UV-2400-PC; Shimadzu, Japan). The results can be seen in Figure 2 (a). For both the AuNP-FB and AgNP-FB cases, we have confirmed very wide extinction spectra with long tails into the IR region, which can be compared with the spectra of the single AuNPs and AgNPs suspensions (before fixation onto the plastic beads). Such a spectral broadening arises from the multipole superradiance of LSPs[13] in densely assembled metallic NPs, which can be understood from theoretical analysis of the discrete integral method with spherical cells (DISC) and the solution of the relevant Maxwell equations.
In particular, we measured time dependence of the temperature at the surface of a PTF with AuNP-FBs and a PTF with AgNP-FBs

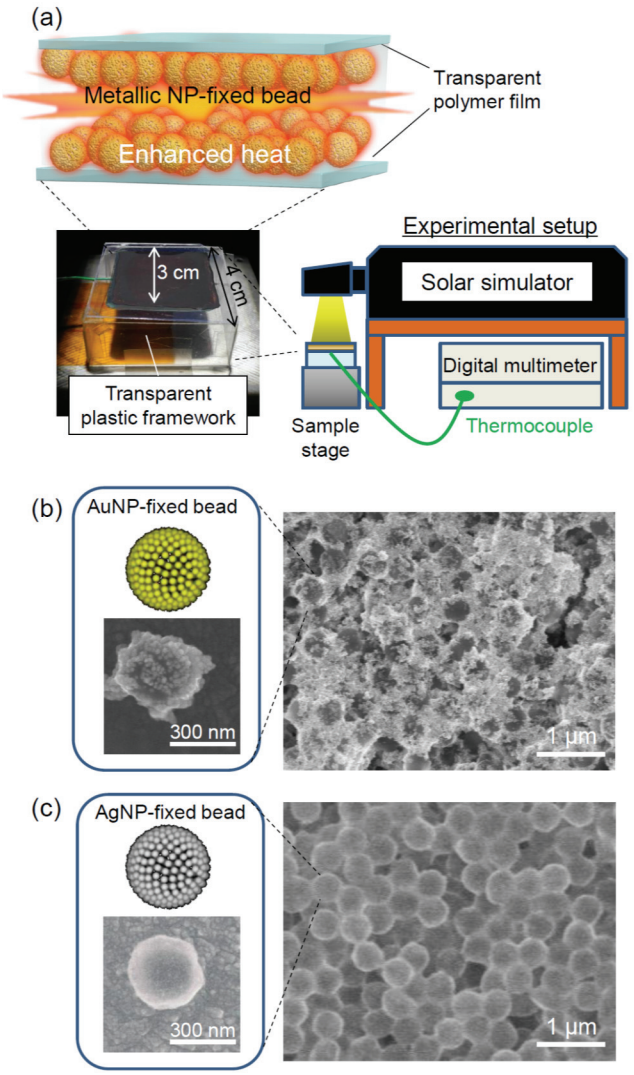

Figure 1. (a) Schematic of experimental setup for determining photothermal effect of metallic nanoparticle-fixed bead (MNFBs) with solar simulator. (b) Scanning electron microscope (SEM) image of Au NP-fixed beads (AuNP-FBs) on transparent polymer substrate after drying. (c) SEM image of Ag NP-fixed beads (AgNP-FBs) on transparent polymer substrate after drying.

under artificial sunlight irradiation, where the initial temperature was set to 25 °C (Figure 2 (b)). The same process was repeated for a PTF with single AuNPs (density in the initial suspension: 6.38 × 10^{11} NPs/mL) and, as a reference, the PEN film with no metallic particles and with black body tape. The results of all five cases are shown together in Figure 2(b). In order to investigate the heat dissipation effect, the temperature of each PTF after the irradiation stopped was also plotted, where the decay can be approximately explained by Newton's law of cooling if the thermal equilibrium is realized. The most notable point is that the temperature of the PTF with the AuNP-FBs reached a peak value of 68.4 °C (temperature change, $\Delta T_{\text{AuNP-FB}}$ = 43.4 °C) after 100 s under artificial sunlight irradiation, which is higher and faster than the temperature rise of asphalt on a road under strong sunlight in midsummer as, typically, a period of approximately 2 h is required for asphalt to reach a

temperature of approximately 60 °C.[17] Also, it has been confirmed that the maximum temperature and speed of temperature rise of PTF with AuNP-FBs is higher and faster than those of PTF with commercial black body tape (XI003B, Yokogawa, Japan) during 100 s irradiation.

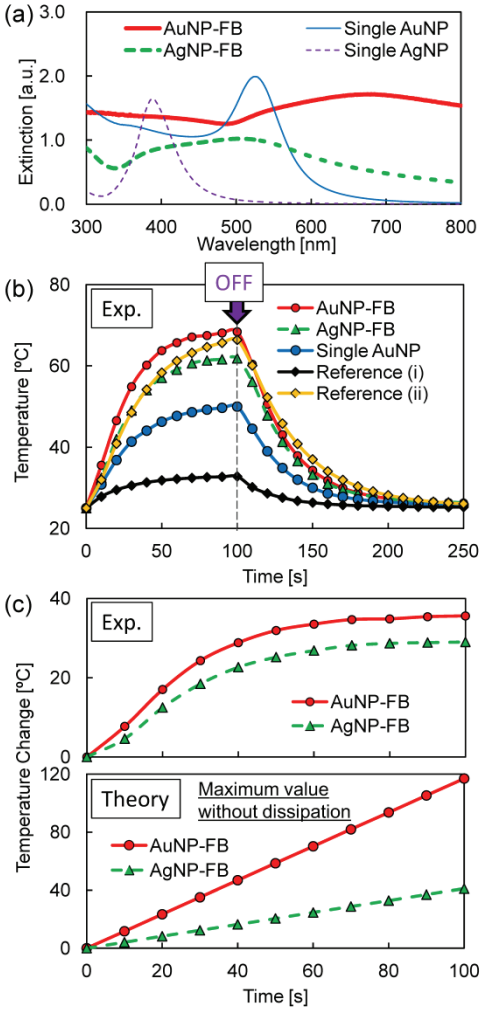

Figure 2. (a) Extinction spectra of aqueous suspensions of AuNP-FBs, single AuNPs before fixation on plastic beads, AgNP-FBs, and single AgNPs before fixation on plastic beads. (b) Irradiation time dependence of temperature of PTFs with AuNP-FBs, AgNP-FBs, single AuNPs, no metallic NPs (Reference (i)), and black body tape (Reference (ii)). The average value of 4 measurements was taken for the respective samples, and the standard deviation of the temperature was less than 1.0 °C. (c) (upper) Observed temperature changes of PTFs with AuNP-FB and AgNP-FBs and (lower) Calculated temperature changes of PTFs without heat loss by the theoretical method in Ref. 13.

In the case of the PTF with AgNP-FBs, the peak temperature was slightly lower, at approximately 61.8 °C ($\Delta T_{AgNP\text{-}FB}$ = 36.8 °C). The final temperatures of the single AuNPs was 50.0 °C (ΔT_{AuNP} = 25.0 °C), while that of the reference PEN film was 32.8 °C (ΔT_{REF} = 7.8 °C). It is worth noting that a previous report using Ag nanocubes and nanoplates mixed on a substrate showed a temperature rise of only 8 °C even after an irradiation period of 30 minutes, which was measured by IR temperature detector[18]. Returning to our results, our developed PTF with AuNP-FBs exhibited $\Delta T_{AuNP\text{-}FB}$ = 29.35 °C even on the TE device after 30 minutes irradiation ($\Delta T_{AuNP\text{-}FB}$ gets lower due to the heat dissipation to the surface of TE device), which was directly measured using a thermocouple connected to a digital multimeter. This result, therefore, indicates that our developed PTF would be much more superior to the previous one[18]. In addition, it was confirmed that the temperature rise ratio (subtracting the reference value) was $(\Delta T_{AuNP\text{-}FB} - \Delta T_{REF})/(\Delta T_{AgNP\text{-}FB} - \Delta T_{REF})$ = 7.73/ 4.63 ≈ 1.67 at 10 s as the initial stage without dissipation, but $(\Delta T_{AuNP\text{-}FB} - \Delta T_{REF})/(\Delta T_{AgNP\text{-}FB} - \Delta T_{REF})$ = 35.6/ 29.0 ≈ 1.23 at 100 s as the final stage. Meanwhile, the ratio of integral values of extinction spectra (from 300 nm to 800 nm) of AuNP-FBs and AgNP-FBs is approximately 1.67 in Figure 2(a). This value seems to be close to the initial temperature rise ratio when the heat dissipation is negligible, whereas it would depend on the difference of dissipation in AuNP-FBs and AgNP-FBs at the final stage of light irradiation. Although the factor of dissipation is complex, these values seem to be consistent. In the case of a PTF with single AuNPs, the final temperature was much lower than that for both the AuNP-FB and AgNP-FB PTFs, even though the AuNP density was the highest under the condition without binder molecule-mediated CSAM. From these results, we can conclude that the observed enhancement in the broadband white light absorption, arising from the collective interaction of LSPs in the respective MNFBs, induced prominently high and rapid temperature rise. In Figure 2 (c) (upper), the temperature change of PTFs with AuNP-FBs or AgNP-FBs was plotted in comparison with the value of the reference (i). Also, in Figure 2 (c) (lower), by the overlap integral of solar spectrum and extinction spectrum of AuNP-FBs or AgNP-FBs but neglecting the heat dissipation effect, the temperature change of PTFs was theoretically evaluated as 117.0 °C corresponding to $\Delta T_{AuNP\text{-}FB} - \Delta T_{REF}$ or 41.0 °C corresponding to $\Delta T_{AgNP\text{-}FB} - \Delta T_{REF}$, respectively (the extinction as a sum of the absorption and the scattering was used since the both factors would affect on the enhancement of heat). The calculation conditions were similar to those in experiment but the heat dissipation was neglected in order to estimate the maximum value during 100 s irradiation (specific heat of typical polymer film ~1.0 J/gK was used). These values are higher than experimental ones and indicate the further enhancement if the heat loss can be suppressed by selecting a material of substrate and so on.

Next, we investigated the possibility of utilizing PTFs with MNFBs in solar TE device applications. Figure 3 (a)-(c) presents a schematic illustration and photographs of our PTF-TE device. Five types of films: AuNP-FBs, AgNP-FBs, single AuNPs, and the reference films (i) with no metallic NPs and (ii) with black body tape, with an active area of ca. 3 × 3 cm^2 were mounted on a ThermoGenerator-Package (TGP) (TGP-651, Micropelt Co. Ltd., Germany) with thermal conductive Si grease (YG6260, Momentive Performance Materials Japan LLC, Japan). The TGP-651 was comprised of a TE device (MPG-651, Micropelt Co. Ltd.,

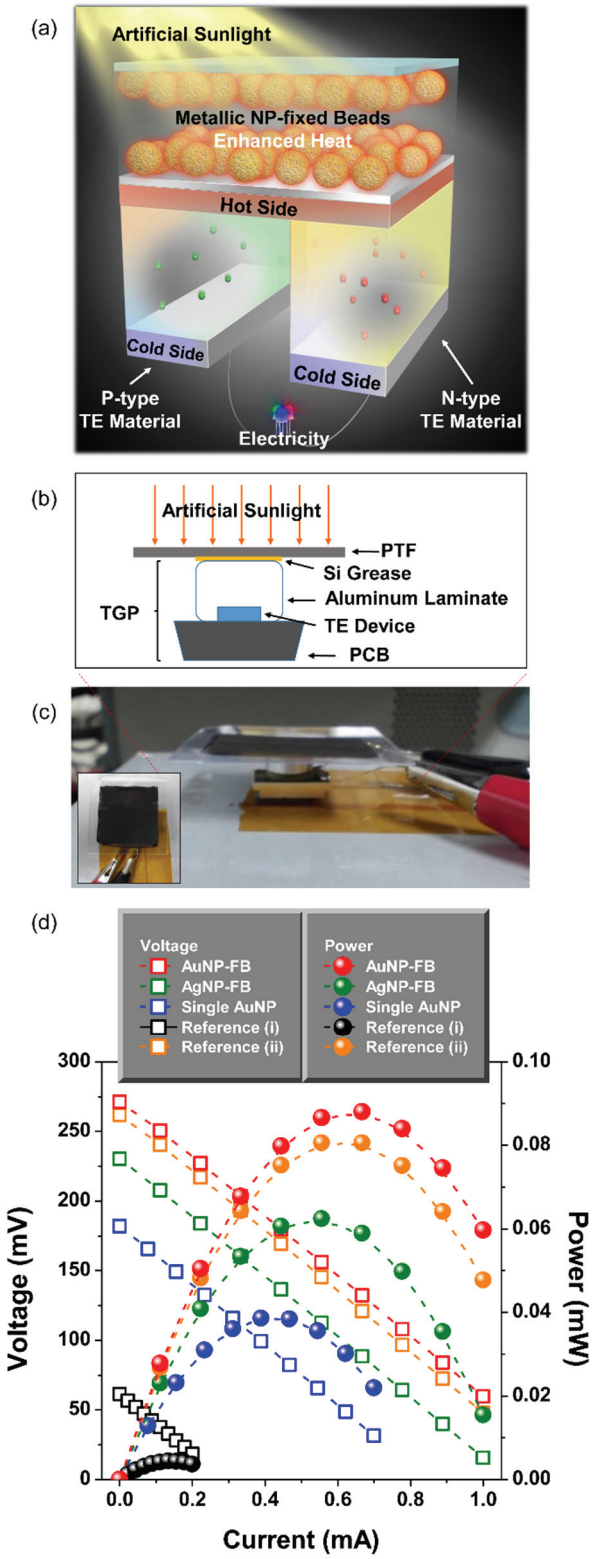

Figure 3. (a) Schematic illustration of solar thermoelectric device based on plasmonic collective phenomena. (b) Structure of PTF-TE device. (c) Photograph of PTF-TE device showing side view (left lower inset: top view). (d) Power generation properties after 5-min simulated sunlight irradiation of PTF-TE devices using AuNP-FBs, AgNP-FBs, single AuNPs, and a reference films (i) with no metallic NPs and (ii) with black body tape, as a PTF. The average values of 4 consecutive measurements per one base current are shown. Error bars are omitted because they were smaller than the symbols shown.

Germany), aluminium laminate with a ring isolator, and a printed circuit board (PCB). The length, width, and thickness of the TGP-651 were 15.0, 10.0, and 9.3 mm, respectively. The MPG-651 was composed of 286 pairs of p-n elements and had a top-side cross sectional-area, bottom-side cross sectional-area, and thickness of ca. 2.5 × 2.5 mm^2, 3.375 × 2.5 mm^2, and 1090 µm, respectively. Measurement of the power generation properties, in which the current-voltage (*I-V*) properties and output power (*P*) were obtained, were carried out in air by changing the load resistance using an electronic load system (low voltage source meter, Keithley 2401, Keithley Instruments Inc., USA) The load resistance was adjusted after 5 min artificial sunlight irradiation of 1 SUN, at AM 1.5 G. Figure 3(d) shows the power generation properties of the PTF-TE device using either the AuNP-FBs, AgNP-FBs, single AuNPs, or the reference films (i) and (ii) as the PTF. The resistance (*R*), open circuit voltage (V_o), maximum output power (P_{max}), and maximum output power density (P'_{max}), are listed in Table S1 (see Electronic Supplementary Information). V_o increased in the following order: reference with no metallic NPs, single AuNPs, AgNP-FBs, reference with black body tape, and AuNP-FBs. According to the Seebeck effect, the temperature difference between a TE device should be proportional to the generated voltage, therefore, this result demonstrated that a PTF with higher performance led to a TE device of higher voltage. P_{max}, defined as V^2/R, also relative to the voltage, and the AuNP-FBs sample showed the highest P_{max} (0.088 mW), which was one order higher than the reference value (0.004 mW). The corresponding P'_{max} value, which is defined as the P_{max} per unit area of the bottom-side cross-sectional area of the TE device, was 1.04 mW cm^{-2}. These results indicate that the differences between the temperature rise of the AuNP-FBs, AgNP-FBs, single AuNPs, and reference films (i) and (ii) in Figure 2 (b) were clearly reflected in the TE measurement, even after a long period of irradiation by artificial sunlight. This fact is promising for PTF design based on controlling the collective effects of LSPs, which depends on the metallic NP density, and will constitute a significant advantage as regards the development of rapid and flexible next-generation solar TE devices.

Author contributions

Sample fabrication: Yo.Y., Shiho.T., Ya.Y., Mo.M., Y.N., K.Y., Shin.T. ; Experiments and data analysis: A. K., Ya.Y., Mo.M., Mi.M., Y.N., K.Y., Shin.T., T.I.; Theory and simulations: Y.N. S.H., T.I.; Manuscript writing and project planning: A.K., T.I.

Acknowledgements

The authors would like to thank Mr. K. Umekage, Mr. M. Tamura, Prof. S. Yagi, Prof. C. Kojima, Prof. H. Shiigi, Prof. T. Nagaoka, and Prof. H. Ishihara for their useful advice and kind support. A major part of this work was supported by the

Special Coordination Funds for Promoting Science and Technology from MEXT (Improvement of Research Environment for Young Researchers (FY 2008-2012)), and Grants-in-Aid for Exploratory Research (No. 24654091 and No. 26610089). T. I. and A. K. contributed equally to this work.

Notes and references

[a] Nanoscience and Nanotechnology Research Center, Osaka Prefecture University, Sakai 599-8570, Japan

[b] Department of Physical Science, Graduate School of Science, Osaka Prefecture University, Sakai 599-8531, Japan

[c] Department of Physics and Electronics, Graduate School of Engineering, Osaka Prefecture University, Sakai599-8531, Japan

[d] GreenChem Inc., Sakai 599-8241, Japan

† Electronic Supplementary Information (ESI) available: Table S1. See DOI: 10.1039/c000000x/

* Corresponding author: t-iida@p.s.osakafu-u.ac.jp, a-kosuga@21c.osakafu-u.ac.jp

1. M. A. Green, in *Solar Cells: Operating Principles,* Technology and System Applications, Univ. New South Wales, 1998.
2. D. M. Rowe, in *Thermoelectric Handbook Macro to Nano*, CRC Press, New York, 2005.
3. M. Telkes, J. *Appl. Phys.*1954, **25**, 765.
4. P. Tomeš, M. Trottmann, C. Suter, M.H. Aguirre, A. Steinfeld, P. Haueter, A. Weidenkaff, *Materials* 2010, **3**, 280.
5. R. Amatya, R. J. Ram, *J. Electro. Mater.* 2010, **39**, 1735.
6. D. Kraemer, B. Poudel, H.-P. Feng, J.C. Caylor, B. Yu, X. Yan, Y. Ma, X. Wang, D. Wang, A. Muto, K. McEnaney, M. Chiesa, Z. Ren, G. Chen, *Nat. Mater.* 2011, **10**, 532.
7. S. Kawata, in *Near-Field Optics and Surface Plasmon Polaritons*, Springer, Berlin, 2001.
8. M.L. Brongersma, P.G. Kik, in *Surface Plasmon Nanophotonics*, Springer, Dordrecht, 2007.
9. H. A. Atwater, A. Polman, *Nat. Mater.* 2010, **9**, 205.
10. T. Iida, J. Phys. *Chem. Lett.* 2012, **3**, 332.
11. S. Ito, H. Yamauchi, M. Tamura, S. Hidaka, H. Hattori, T. Hamada, K. Nishida, S. Tokonami, T. Itoh, H. Miyasaka, T. Iida, *Sci. Rep.* 2013, **3**, 3047.
12. Y. Yamamoto, S. Takeda, H. Shiigi, T. Nagaoka, *J. Electrochem. Soc.* 2007, **154**, D462.
13. S. Tokonami, S. Hidaka, K. Nishida, Y. Yamamoto, H. Nakao, T. Iida, *J. Phys. Chem. C* 2013, **117**, 15247.
14. S. Tokonami, K. Nishida, S. Hidaka, Y. Yamamoto, H. Nakao, T. Iida, *J. Phys. Chem. C* 2014, **118**, 7235.
15. C. Kojima, Y. Watanabe, H. Hattori, T. Iida, *J. Phys. Chem. C* 2011, **115**, 1909.
16. Y. Nishimura, K. Nishida, Y. Yamamoto, S. Ito, S. Tokonami, T. Iida, *J. Phys. Chem. C* 2014, 118, 18799.
17. M. Nishioka, M. Nabeshima, S. Wakama, J. Ueda, *J. Heat Island Instit. Internat.* 2006, **1**, 46.
18. Y. Xiong, R. Long, D. Liu, X. Zhong, C. Wang, Z.-Y. Lib, Y. Xiea, *Nanoscale* 2012, **4**, 4416.